

*Full Length Research Paper*

# **A comparative analysis of MODIS-derived drought indices for Northern and Central Namibia**

**Daniel Wyss<sup>1\*</sup>, Kaleb Negussie<sup>2</sup>, Antonia Staacke<sup>1</sup>, Amadé Karnagel<sup>1</sup>, Malin Engelhardt<sup>1</sup> and Martin Kappas<sup>1</sup>**

<sup>1</sup>Department of Cartography, Faculty of Geoscience and Geography, GIS and Remote Sensing, Georg-August-Universität Göttingen (GAU), Germany.

<sup>2</sup>Department of Geo-Spatial Sciences and Technology, Faculty of Natural Resources and Spatial Sciences, Namibia University of Science and Technology (NUST), Namibia.

Received 1 February, 2022; Accepted 4 May, 2022

**Namibia is a semi-arid country with erratic and unpredictable rainfall. Extreme weather patterns, such as floods and extensive droughts, have become more common in recent years, with strong impact on surface and ground water availability, rangeland and agricultural productivity, food security, and further land degradation, such as bush encroachment or soil erosion. The previous 10 years were characterized by a perennial drought that lasted from 2013 to 2016 and an extreme drought that occurred during the rainy season of 2018/2019, which was the driest in 90 years. In January 2021, however, rainfall totals doubled to tripled the norm. The paper compares five drought indices in order to identify, visualize, monitor, and better understand the nature, characteristics, and spatial-temporal patterns of drought in northern and central Namibia. Based on their sensitivity to vegetation greenness, land surface temperature, evapotranspiration, and precipitation, the indices allow for calculation, time series analysis, and cross-comparison. Droughts occur every year, but the intensity of the drought varies depending on the index type. It is concluded that a comparative analysis of multiple indices provides a better interpretation of drought than single parameter systems. Future research should include biophysical properties such as soil characteristics, soil moisture, and hydrology, as well as socioeconomic studies, in order to develop an integrated drought index for northern Namibia.**

**Key words:** Remote sensing, moderate resolution imaging spectroradiometer (MODIS), drought indices, time series analysis, climate reanalysis, Namibia.

## **INTRODUCTION**

Droughts are extreme climate phenomena characterized by significantly lower than normal precipitation levels over a prolonged period of time, resulting in water scarcity (Haroon et al., 2016; Mishra and Singh, 2010). These recurring natural hazards occur worldwide, cause hydrological imbalances, and can have serious negative impacts in

many sectors of society if the conditions persist for an extended period of time (Tadesse, 2016). Climate change has resulted in a significant increase in mean global surface temperatures, resulting in extreme climatic conditions such as droughts caused by low precipitation over months or years in a specific area (Valejo Orti and Negussie, 2019). These natural

\*Corresponding author. E-mail: [daniel.wyss@uni-goettingen.de](mailto:daniel.wyss@uni-goettingen.de).

disasters affect millions of people in Sub-Saharan Africa, causing malnutrition, water scarcity, and increased urbanization as a result of increased rural-urban migration. The same is true for Namibian rural communities that rely primarily on subsistence agriculture and livestock farming. The expected increase in exceptional droughts as a result of late and poor rainfall performance will have a significant impact on agricultural productivity, grazing capacity, and water availability, with serious consequences for rural health and household food security.

Precipitation is one of the most important parameters for determining water availability and the likelihood of drought. Namibia's annual rainfall shows a distinct gradient from north (~600 mm) to south (~300 mm) due to its location within the subtropical high-pressure zone. There is also a distinct precipitation gradient from the coast to the north-eastern parts of the country, ranging from 25 mm in the southwest to 700 mm in the northern Zambezi region. During the rainy season (October to April), the country is characterized by long dry periods and short episodes of abundant and highly erratic rainfall caused by a shift in the ITC zone or by the periodic El Niño- and La Niña-Phenomena (Mendelsohn, 2009). These phenomena are expected to cause agricultural drought every three years, as well as decennial flood events. Rainfall is expected to fall across the country, particularly in the central and northwest. Furthermore, temperatures are expected to rise (Orti und Negussie, 2019). The National Climate Change Strategies and Action Plan 2013-2020 also confirms an increase in prolonged and more severe droughts and floods, with an expected decline in soil moisture, increased evapotranspiration, low groundwater recharge, and decreased water availability in both quantity and quality.

According to FloodList Namibia ([www.floodlist.com](http://www.floodlist.com)), severe flooding events, particularly in the Cuvelai-Etoshia-Basin, were recorded in 2011, 2013, 2014, 2020, and 2021. Between 2013 and 2016, a persistent meteorological drought phase occurred, culminating in an extreme drought during the 2018/2019 rainy season. Windhoek received the least amount of rain in 2019 since 1891, and Namibia received the least amount of rain in 90 years. The drought affected over 500,000 Namibians, killed over 60,000 livestock, and left residents facing food insecurity and water shortages (Shikangalah, 2020). In contrast, January 2021 saw the highest rainfall totals since the rainy season of 2010/2011, with precipitation reaching a country-wide average of 268 mm (NOAA Climate prediction center), with extreme rainfall events in Namibia's north-eastern, central, and southern regions.

Proposed strategies to mitigate these impacts, according to the National Climate Change Strategies and Action Plan, include improving understanding of climate change and related policy responses, using monitoring and data collection technologies for surface and ground water at the basin/watershed level, and promoting conservation and sustainable use of water resources (Rensburg and Totajada, 2021).

Drought monitoring is an important task for guiding

appropriate response measures by monitoring the changing dynamics of soil, water, and vegetation cover. Early detection of droughts has the potential to mitigate negative effects on water resources and the agricultural sector. Drought detection is possible using satellite imagery and derived products at various resolutions, allowing for detailed as well as supra-regional time series analysis and monitoring. Understanding the interaction of environmental parameters and vegetation cover is critical for planning and management, particularly in more sensitive semi-arid regions where extensive research has been conducted in recent years (Sandeep et al., 2020; Sardooi et al., 2021; Angearu et al., 2020; Vova et al., 2019). Droughts are typically classified into four types: (1) Meteorological droughts characterized by precipitation deficits; (2) Agricultural droughts characterized by reduced crop production and availability of forage for livestock due to unreliable rainfall and soil moisture deficits (Dalezios et al., 2017; Gidey et al., 2018); (3) Hydrological droughts characterized by low stream flow and ground water levels; and (4) Socioeconomic droughts characterized by water supply and social response (Keyantash and Dracup, 2002; AghaKouchak et al., 2015). Droughts can be measured in terms of their onset, extent, duration, and magnitude (Kogan, 1995), but the spatial and temporal variability of each event is difficult to quantify. Drought is also a very complex phenomenon that is dependent on various interactions of hydrological parameters such as precipitation, evapotranspiration, runoff, infiltration, surface and groundwater storages (Kim et al., 2017).

There are numerous methods for mapping and monitoring drought based on more than 100 existing drought indicators (selected indices are presented in Table 1). This makes choosing the right indicator for a specific situation or region extremely difficult. Most drought indicators have a limited scope, focusing on individual indicators that show comparable signals (Naumann et al., 2014) and thus ignoring other important determinants.

Although precipitation, as measured by the derived Standardized Precipitation Index (SPI) or the Standardized Precipitation Evapotranspiration Index (SPEI), is the best observed variable for characterizing meteorological drought on a variety of timescales (Angearu et al., 2020), it cannot adequately characterize drought conditions in specific study areas. Soil moisture, land surface temperature, evapotranspiration, greenness-based indices, and socioeconomic indicators must also be considered, as they can meaningfully supplement each other (Du et al., 2018; Luetkemeier et al., 2017; Zargar et al., 2011; Mukherjee et al., 2018). The Normalised Difference Vegetation Index (NDVI) is a commonly used index for drought monitoring, particularly in semi-arid environments with less than 30% vegetation cover (Sandeep et al., 2020). Gross Primary Production (GPP), Leaf Area Index (LAI), Vegetation Condition Index (VCI), and Enhanced Vegetation Index (EVI) are other commonly used indices (EVI) (West et al., 2019).

Different institutions in Namibia coordinate early

**Table 1.** Selection of globally used drought indices.

<b>S/N</b>	<b>Conventional data-based drought indices</b>
1	Agricultural Drought Index (DTx)
2	Bhalme-Mooley Drought Index (BMDI)
3	Corn Drought Index (CDI)
4	Crop Moisture Index (CMI)
5	Crop Specific Drought Index
6	Evapotranspiration Deficit Index (ETDI)
7	Global Vegetation Water Moisture Index (GVWI)
8	Leaf Water Content Index (LWCI)
9	Moisture Availability Index (MAI)
10	Reclamation Drought Index (RDI)
11	Soil Moisture Anomaly Index (SMAI)
12	Soil Moisture Deficit Index (SMDI)
13	Soil Moisture Drought Index (SMDI)
14	Standardized Vegetation Index (SVI)
15	Computed Soil Moisture
16	Agro-Hydro Potential
	<b>Satellite data-based drought indices</b>
1	Normalized Difference Vegetation Index (NDVI) (Tucker, 1979)
2	Deviation NDVI index
3	Enhanced Vegetation Index (EVI)
4	Vegetation Condition Index (VCI) (Kogan, 1995)
5	Monthly Vegetation Condition Index (Kogan, 1995)
6	Temperature Condition Index (TCI) (Kogan, 1995)
7	Vegetation Health Index (VHI)
8	Normalized Difference Temperature Index (NDTI)
9	Crop Water Stress Index (CWSI)
10	Drought Severity Index (DSI)
11	Temperature- Vegetation Dryness Index (TVDI)
12	Normalized Difference Water Index (NDWI)
13	Remote Sensing Drought Risk Index (RDRI)
14	Vegetation Drought Response Index (VegDRI)

warning and drought monitoring, including the Ministry of Agriculture, Water and Forestry (MAWF), Namibia Meteorological Services (NMS), and the Directorate of Disaster Risk Management, which report on agricultural productivity, livestock and pasture conditions, household food security, water availability, seasonal rainfall outlooks, and drought-affected geographic areas. Despite previous severe droughts, research on the use of remotely sensed indices for drought monitoring in Namibia remains limited. A study presented through the CuveWaters project that presents a blended drought index (BDI) as an integrated tool for drought impact estimation in the semi-arid Cuvelai-Basin of Angola and Namibia is an exception. It takes into account meteorological and agricultural droughts, as well as the population's sensitivities and coping abilities (Luetskemeier et al., 2017). A paper on precipitation and vegetation correlation analysis using SPI and SVI (Standardized Vegetation Index) indices to assess long-term climate and vegetation changes for Namibia was recently

published (Liu and Zhou, 2021). Other publications concentrate on policies and social impacts of drought that is, the assessment of the 2015-2017 droughts in Windhoek from the perspective of drought management and governance (Rensburg and Tortajada, 2021). The existing rangeland monitoring project in Namibia is a first step toward an integrated Drought Monitoring System (DMS), with the goal of developing and testing a rangeland early warning and monitoring system for improved decision making with selected farming communities, ranchers, and other stakeholders (Namibia-rangelands.com). The project, which has been in operation since 2015, was funded by the European Union's Climate Change Adaptation and Mitigation program.

During the rainy season, it provides drought maps on a national and regional scale every 10 days. These are solely based on the NDVI vegetation product from the MODIS (Moderate Resolution Imaging Spectroradiometer), including NDVI deviation from mean and VCI. In addition, useful tools such as

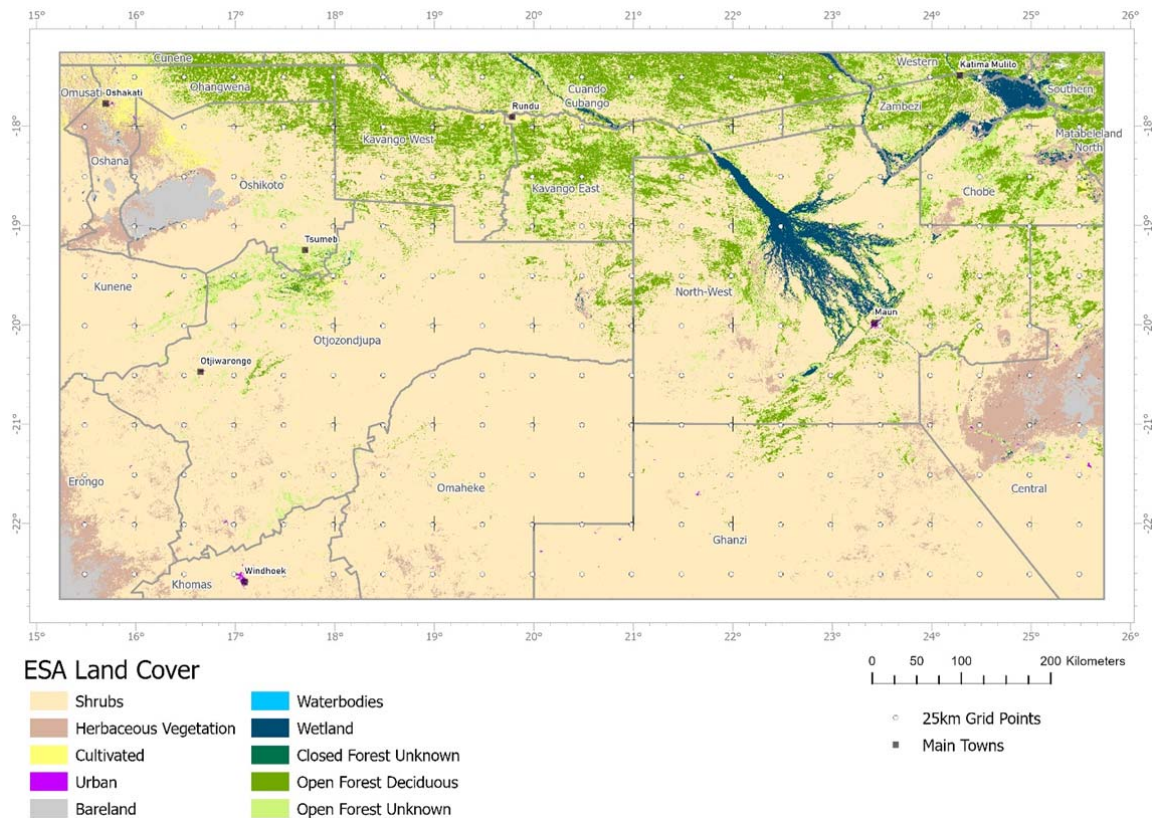


**Figure 1.** Study area and land cover based on ESA Copernicus Global Land Service in a 100 m spatial resolution containing 25 km grid points for further spatial and statistical analysis of drought index values.

regional greenness statistics or a fodder flow planer, to estimate herbaceous biomass available at the end of the rainy season, are provided. An additional useful tool to monitor droughts on a supra-regional level is the operational African Drought and Flood Monitor (ADFM), which was developed by UNESCO and Princeton University (US) in 2011. The ADFM monitors and forecasts meteorological and hydrological drought using merged reanalysis and observational *in-situ* meteorological data, providing a hydrological modeling platform and accompanying web-based user interface. In the meantime, a more tailored, national version of the Monitor has been developed for Namibia to strengthen flood and drought risk management in the country. To address disaster risk reduction, a first participatory workshop on flood and drought monitoring was held in July 2021. The web application provides real-time meteorological parameters but is limited to macroscale analysis due to the relatively low spatial resolution of five kilometers. There have been no published studies comparing MODIS-based drought indices. To fill this void, this study compares five MODIS-based drought indices over the last decade to visualize and quantify spatiotemporal drought dynamics and affected areas. These include NDVI-based indices as well as combined indices that incorporate MODIS evapotranspiration and temperature data. The cross-correlation of selected indices and their comparison to

climate reanalysis data is a novel application for northern and central Namibia, which are characterized by semi-arid conditions and a highly erratic rainfall regime.

### Study area

Figure 1 shows the study area from 16 to 26° longitude and 20 to 17° latitude. The total area is approximately 670,000 km<sup>2</sup> and it includes some of Namibia's northern communal regions (Oshana, Oshikoto, Kavango and Zambezi), where subsistence agriculture is predominant, the Otjozondjupa Region, and parts of the Erongo, Kunene, Omaheke, and Khomas Regions of central Namibia. The rectangular extent of the study area also includes parts of Angola (Cubango region), as well as Botswana (Northwest, Chobe, Ghanzi and Central regions), covering various landscapes and allowing for cross-boundary analysis. According to Mendelsohn's Atlas of Namibia (2009), the chosen extent covers six predominant landscapes of Namibia: The Kamanjab Plateau, Karstfeld, the Cuvelai System with the Etosha salt pan, Central Western Plains, Kalahari Sandveld and the Caprivi Floodplains (from West to East), including catchments of the Okavango river shared between Angola, Namibia, and Botswana, and the Omuramba-Omatako rivers stretching from

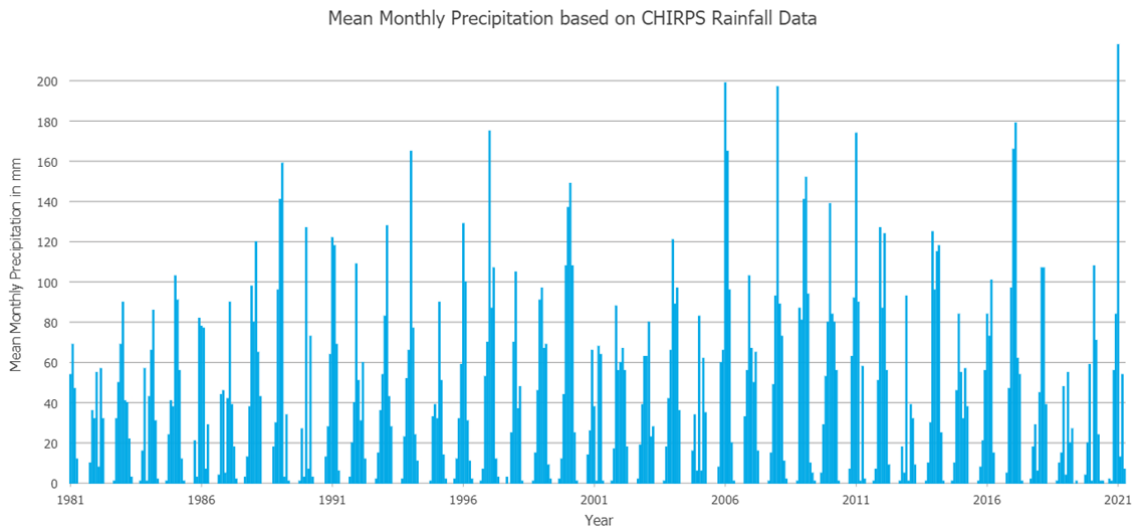


**Figure 2.** Mean monthly precipitation based on CHIRPS (Climate Hazards Group InfraRed Precipitation) rainfall estimates.

north-eastern to central Namibia. Prominent landscapes of Botswana include the Okavango delta and the Makadikgadi salt pans situated in dry savanna southeast of the Okavango delta. The area is generally sparsely populated but includes areas of high population density, especially within the northern Omusati, Oshana and Ohangwena regions. Apart from Windhoek (Khomas region), larger towns with a population of ~60 thousand are Rundu and Maun. Oshakati, Katima Mulilo, Otjiwarongo and Tsumeb have population numbers between 20 and 40 thousand (Republic of Botswana, 2012; Namibia Statistics Agency, 2012).

The rainfall gradient of the study area from northeast to southwest has an effect on the vegetation structure. The vegetation is primarily tree and shrub savanna. In the north, open woodlands give way to shrubland-woodland mosaics in the east and dense shrub lands in the center. The land cover classification depicted in Figure 1 is based on a subset of ESA Copernicus Global Land Service data at a resolution of 100m [Buchhorn et al., 2020], and it depicts primarily shrubland with open forests in the north, as well as wetlands (Zambezi, Okavango delta) and herbaceous vegetation surrounding the Etosha and Makadikgadi salt pans. Open woodland accounts for approximately 16% of the total area, while shrub land accounts for 74%. The remaining 10% is divided into wetland (2%), bare land (1.5%), and herbaceous vegetation (5%), with cultivated and urban areas accounting for only 1.5 percent of the total. The study area is also divided into a 25km grid with centroids per grid cell for further spatial and statistical analysis via index value extraction.

Figure 2 illustrates the highly variable amounts of precipitation in the study area over a 30-year time period (1981 to 2021) using CHIRPS (Climate Hazards Group Infrared Precipitation) global rainfall data at 1-

month temporal resolution based on rainfall estimates from gauge and satellite observations (Funk et al., 2015). The graph covers the time-period from 1981 to 2021, and clearly indicates the perennial meteorological drought conditions during the rainy seasons (October until April) of 2012/13 to 2015/16, as well as the extreme drought season of 2018/19, with a mean precipitation of only 175 mm. Drier conditions can also be observed in the early 1980's (1981 to 1987). The 2019/2020 season had higher mean rainfall values (285 mm), which increased significantly to 430 mm in 2020/21, according to CHIRPS data. Other seasons with above-average rainfall amounts include 2010/2011 with 480 mm and 2005/2006 with a maximum of 613 mm.

The data were accessed using Google Earth Engine (GEE) and a JavaScript provided by the UN-Spider knowledge portal ([www.un-spider.org](http://www.un-spider.org)), which allows for the estimation of rainfall variations in space and time as a key component of drought early warning and environmental monitoring. In recent years, the CHIRPS dataset has been used as a replacement for ground-based precipitation data (Rivera et al., 2019; Gao et al., 2018).

## DATA AND METHODS

A network of Southern African Science Service Centre for Climate Change and Adaptive Land Management (SASSCAL) weather stations was initiated in 2009/2010 to record spatial climatic variability throughout the SADC region. These provide valuable *in-situ* measurements of climatic variables but lack consistency in respect to measurement data due to different implementation dates, missing values, and sparse spatial coverage. The same applies to the meteorological data provided by the Ministry of Environment and Tourism (MET) in Namibia. For time series analysis, meteorological data in adequate spatial and timely resolution is necessary. As such, this study incorporates precipitation reanalysis data for later cross-

comparison with derived drought indices. There are numerous global reanalysis rainfall datasets available. The Copernicus Climate Change Service, in addition to CHIRPS, GPCC (Global Precipitation Climatology Centre), MERRA (Modern-Era Retrospective Analysis for Research and Applications), and TerraClimate, provides ERA-5 data produced by the European Centre for Medium-Range Weather Forecasts (ECMWF). The ERA-5 data sets provide climatic variables in a 0.25° resolution. All four datasets show good levels of correlation and also correlate well with data provided through the operational SASSCAL weather stations (Karnagel, 2020; Engelhardt, 2021). ERA-5 showed the highest overall correlation and has therefore been used for further analysis. ERA-5 monthly averaged precipitation data was downloaded from the Copernicus Climate Data Store (CDS) and processed as NetCDF (Network Common Data Form) multidimensional data to produce seasonal rainfall composites for the past 10 years (2011 to 2021).

Drought indices were calculated using MODIS spectral reflectance imagery and pre-processed data products. The MODIS instrument, which is installed on the American Terra and Aqua earth observation satellites, has a viewing swath of 2,330 km and a high temporal resolution, acquiring imagery every one to two days. (Thenkabail et al., 2004). The sensor serves as a successor to the Advanced Very High-Resolution Radiometer (AVHRR) to monitor terrestrial ecosystems for the National Aeronautics and Space Administration (NASA), and acquires data in 36 spectral bands with spatial resolutions between 250 m and 1 km (Persendt, 2009).

The products are distributed through the Land Processes Distributed Active Archive Center (LP DAAC) in various processing levels and generally utilize the sinusoidal grid tiling system. The following MODIS products were processed using MODISstp, which is an R-package allowing automated download and pre-processing (mosaicking, sub-setting and reprojection) of single MODIS tiles to produce time series of MODIS land products. For the past 20 years (2001 to 2021), products were processed for the growing season (November to April) and re-sampled to a common spatial resolution of 500 m and re-projected to a Geographic Coordinate System (GCS, WGS 84).

1. Vegetation Indices product (16-Day composite, 500 m spatial resolution, MOD13A1);
2. Land Surface Temperature product (8-day composite, 1 km spatial resolution, MOD11A2);
3. Net Evapotranspiration product (8-day composite, 500 m spatial resolution, MOD16A2);
4. Surface Reflectance product (8-Day composite 500 m spatial resolution, MOD09A1).

The Vegetation Indices (VI) product includes seven bands, with different waveband centres, as well as already computed indices (e.g. NDVI and the Enhanced Vegetation Index - EVI) based on algorithms for the best available pixel values without clouds. These can potentially link climate changes (e.g. increasing frequency and severity of drought) and vegetation responses to land-atmosphere water, carbon, and energy fluxes (Huete et al., 2011). The Land Surface Temperature (LST) product contains averaged LST and emissivity values that are generated from the thermal infrared bands (Hulley et al., 2016). LST is an important environmental variable in drought monitoring, and when combined with NDVI, valuable information for describing agricultural drought for early warning systems can be derived (Zhang et al., 2017). The Net Evapotranspiration (ET) product uses the Penman-Monteith equation to calculate evapotranspiration and contains the sum of lost water due to evaporation from the soil surface and transpiration from plants growing on it over an eight-day period in kg per m<sup>2</sup>. The product also contains Potential Evapotranspiration (PET), indicating the amount of evaporation in kg per m<sup>2</sup> that would occur if a sufficient water source would be available. The ratio of ET to potential ET (PET) is commonly used as an indicator of terrestrial water availability and associated wetness or drought (Running et al., 2019).

In addition, Surface Reflectance products (SF) were downloaded and processed to create MODIS composite images for selected rainy seasons. Figure 3 shows selected MODIS false natural color composites based on 8-day MODIS surface reflectance products in a 500 m spatial resolution. The composites for the past three growing seasons, 2018/2019 to 2020/2021, are compared to NDVI deviation maps from long-term mean values, clearly showing the spatial-temporal patterns of vegetation health in the study area. During the 2018/2019 extreme drought season, vegetation stress is clearly visible, affecting riparian vegetation along the Okavango delta's fringes as well as shrub savanna in central Namibia (Otjizondjupa and Khomas regions) south of the Etosha salt pan. Increased precipitation during the following growing seasons results in a constant greening of vegetation, as well as the ephemeral transformation of dry salt pans into wet landscapes covered by a thin layer of water. Figure 4 depicts some of the MODIS composite products that were used in this study to calculate drought indices.

The value range of NDVI is generally -1 to 1 with negative values corresponding to water, values close to zero corresponding to barren areas, while high values indicate temperate and tropical rain forests (www.usgs.gov). Mean NDVI values for the study area show a constant increase from 0.37 in 2018/2019 to 0.42 in 2019/2020 and 0.49 in 2020/21, respectively. Maximum mean values of > 0.7 are typically found in the Okavango Delta, in the northern open forests, and the Zambezi region, while salt pans (bare land) and herbaceous vegetation indicate lowest mean NDVI values with a minimum value of -0.03 in 2018/2019. Mean LST values have decreased from 40°C in 2018/19 to 33°C in 2020/21, with a maximum value of 52°C indicating a typical negative correlation between NDVI and LST.

Mean ET values increase with vegetation greenness and moisture content and positively correlate with NDVI. ET increased from 5.4 kg per m<sup>2</sup> in 2018/2019 to 16.2 kg per m<sup>2</sup> in 2020/21, with a maximum value of 45 kg per m<sup>2</sup>. NDVI, LST and ET follow distinct spatial patterns, with the lowest NDVI and ET values and the highest LST values in the central region of Botswana, as well as in Erongo, Oshakati, and Oshana regions of Namibia. The above products yielded five widely used drought indices. These include the greenness-based Vegetation Condition Index (VCI), the temperature-based Temperature Condition Index (TCI) as well as the combined indices: Vegetation Health Index (VHI), Drought Severity Index (DSI), and the Temperature Vegetation Dryness Index (TVDI). Apart from TVDI, all indices are computed in a similar way by comparing a current time stamp such as a month or season with mean, minimum or maximum values of the total time series. The time series within this study is based on mean NDVI, LST and ET/PET values covering a 20-year time period (2001 until 2021) concentrating on annual growing seasons from November until April. VCI, VHI and DSI include the MODIS NDVI product which was developed by Tucker in 1979. NDVI is used to assess the vitality and expression of vegetation and is formed through the quotient of spectral reflectance measurements acquired in the visible red ( $\lambda_{red}$ ) and near-infrared regions ( $\lambda_{NIR}$ ). The calculation assumes that radiation in  $\lambda_{red}$  is strongly absorbed by vegetation chlorophyll and radiation in  $\lambda_{NIR}$  is strongly reflected by healthy vegetation. As vegetation vitality decreases, reflection increases in the  $\lambda_{red}$  spectral range and decreases in  $\lambda_{NIR}$ . NDVI is calculated as follows (Thenkabail et al., 2004):

$$NDVI = \frac{\lambda_{NIR} - \lambda_{red}}{\lambda_{NIR} + \lambda_{red}}$$

VCI was suggested by Kogan in 1995 and calculates the impacts of drought on vegetation and its severity by noting vegetation changes and comparing them with historical minimum and maximum NDVI values. Low index values indicate stressed vegetation, with NDVI close to its long-term minimum, and high values representing above normal conditions, indicating healthy vegetation conditions (Anyamba and Tucker, 2012). A threshold

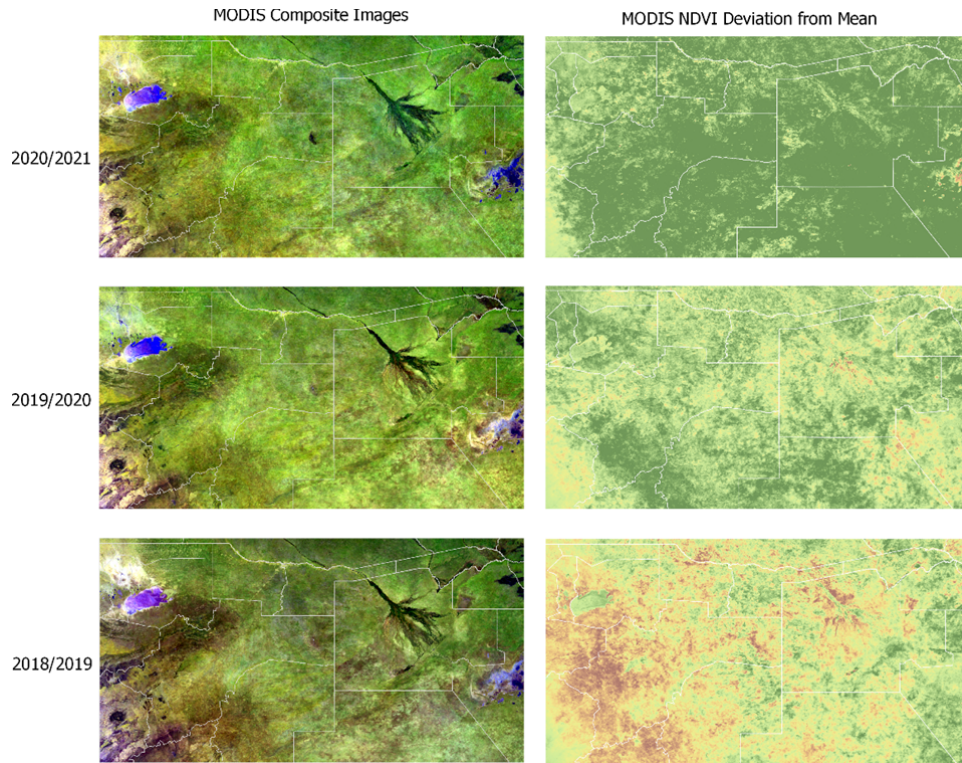


**Figure 3.** Comparison of MODIS rainy season image composites based on 8-day MODIS Surface Reflectance products as ‘False Natural Color’ representations (left) and MODIS NDVI 500 m deviation from mean products based on a 20-year NDVI time series.

of 40% is used to identify droughts (Winkler et al., 2017) after calculating VCI as shown:

$$VCI = \frac{NDVI - NDVI_{min}}{NDVI_{max} - NDVI_{min}} * 100$$

Over the years, several indices based on satellite thermal infrared (TIR) data have been developed, such as TCI, which works similarly to VCI but uses LST data as input, and TVDI, which is discussed further below. The index can be used to determine temperature related vegetation stress and estimate soil moisture content. TCI identifies vegetation stress caused by high temperature, as well as excessive wetness. Low TCI values indicate hot weather and, over a longer period, they indicate droughts (Karnieli et al., 2006). LST is computed from thermal infrared (TIR), bands providing a direct measure of surface temperature and an indirect estimate of moisture availability (Du et al., 2018). The same threshold value as VCI is used to identify droughts. The index is produced using the formula:

$$TCI = \frac{LST_{max} - LST}{LST_{max} - LST_{min}} * 100$$

VHI is a widely used remote sensing-based agricultural drought index designed as the weighted sum of VCI and TCI. It is considered as a robust index, especially for arid, semi-arid, and sub-humid climatic regions (Gidey et al., 2018). The first component characterizes moisture conditions and is typically based on information from the visible and near infra-red windows of the electromagnetic spectrum, whereas the latter characterizes the thermal condition and is based on information from the thermal infra-red window. The combination of both indices represents overall vegetation health and has a stronger relationship with soil moisture than VCI or TCI alone. The index

should only be used if NDVI and LST correlate negatively (Karnieli et al., 2010). The inverse correlation indicates that vegetation cover reduces LST and increases the ratio of LST/NDVI during drought [Solangi et al., 2019]. The optimal weights for VCI and TCI are typically unknown, and VHI is typically estimated by assuming equal weights of 0.5 for both components. Droughts are identified using the same threshold value as VCI and TCI:

$$VHI = 0.5 * VCI + (1 - 0.5) * TCI$$

The DSI, developed by MU et al. (2013), is a standardized index that has proven to be reliable for studying agricultural droughts as well as identifying meteorological droughts (Khan and Gilani, 2021). The index uses the ratio of ET and PET products including standardized NDVI values (Haroon et al., 2016). The ratio of ET to PET is used as an indicator of terrestrial water availability indicating particularly wet or dry conditions, but is also related to carbon and energy cycles of the land surface and can thus be used to assess vegetation response to drought. To obtain normalized Z-values for each rainy season, the mean values (M) and standard deviations (SD) of the ET/PET (Z1) and NDVI (Z2) ratios were calculated for the entire time series. The DSI was then calculated by combining the Z of each rainy season with the mean and standard deviations of the Z of the entire time series:

$$Z1 = \frac{\frac{ET}{PET} - \frac{ET}{PET}_M}{\frac{ET}{PET}_{SD}}$$

$$Z2 = \frac{NDVI - NDVI_M}{NDVI_{SD}}$$

$$Z = Z1 + Z2$$

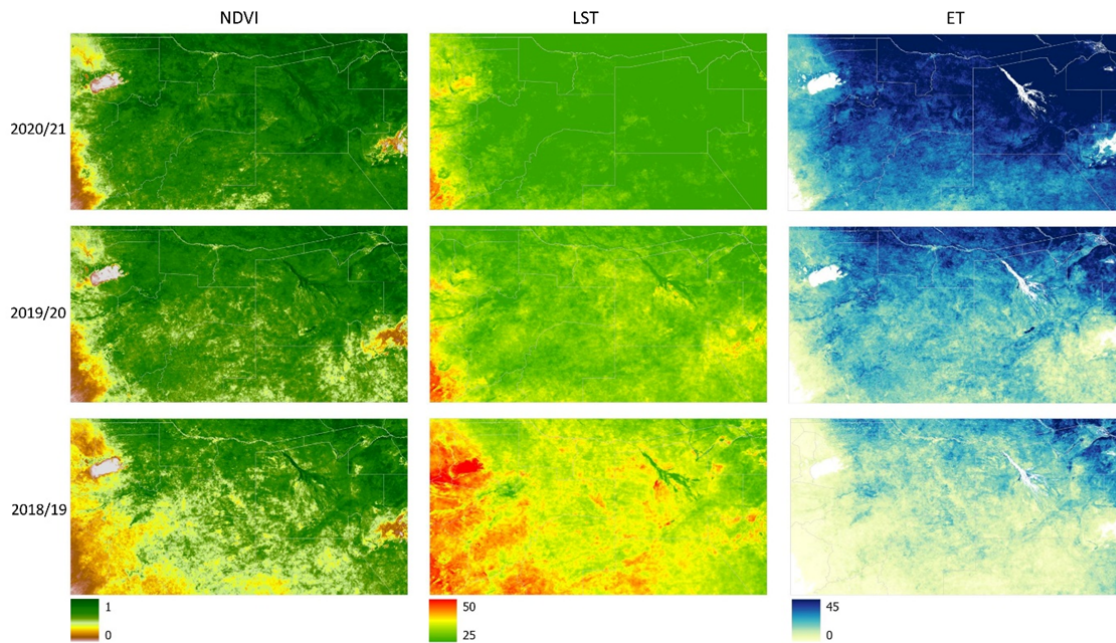


**Figure 4.** Comparison of mean MODIS NDVI values indicating values between 0 and 1 (left), LST with values between 25 and 50°C (middle) and ET products with values between 0 and 45 kg per m<sup>2</sup> (right) during the past three rainy seasons.

$$DSI = \frac{Z - Z_M}{Z_{SD}}$$

The index is dimensionless and thus has an infinite positive and negative range of values. Negative values represent drier than normal conditions, whereas positive values indicate wetter conditions. Thresholds of less than or equal to -1.5 characterize extremely dry conditions, and thresholds greater than or equal to 1.5 show extremely wet conditions (Mu et al., 2013).

TVDI is a simplified temperature vegetation dryness index which has been commonly implemented to estimate regional soil moisture in arid and semi-arid regions (Tao, 2021). The index is determined by the relationship between the NDVI and LST values for the same pixel.

$$TVDI = \frac{T_s - T_{smin}}{T_{smax} - T_{smin}}$$

T<sub>smax</sub> and T<sub>smin</sub> can be represented by a straight-line relationship of temperature and NDVI, and can be drawn in a scatterplot, in which minimum LST values represent the wet edge and maximum LST values represent the dry edge (Sandholt et al., 2002). To obtain these values, the minimum and maximum temperatures of the study area are calculated for each growing season and then related to NDVI. The regression constant *a* and regression coefficient *b* are calculated for both minimum and maximum temperatures in conjunction with the average NDVI for the growing season (Ali et al., 2019). According to Lu et al. (2007), the TVDI value range is 0 to 1 and is divided into five classes: wet (0-0.2), average (0.2-0.4), mild drought (0.4-0.6), moderate drought (0.6-0.8), and severe drought (0.8-1.0).

$$T_{smax} = a_1 + b_1 * NDVI$$

$$T_{smin} = a_2 + b_2 * NDVI$$

## RESULTS

SPI is a widely used index to characterize

meteorological drought and is recommended by the World Meteorological Organization (WMO). SPI is simple to calculate since it is solely based on precipitation data. Long-term precipitation records of 20 to 30 years are compared to the current rainfall of any location or region producing a standardized deviation from normal (McKee et al., 1993). SPI index values are either positive, indicating wet conditions or negative indicating dry conditions. Figure 5 shows the high variability of mean monthly SPI versus 16-day mean NDVI values for the study area over a 20-year period (01.01.2001 to 16.10.2021) using GEE JavaScript code and CHIRPS data. In semi-arid regions, precipitation is the main limiting factor for vegetation growth. Vegetation is greatly sensitive to climate change, and abnormal changes in precipitation during the growing season can further exacerbate the occurrence of drought (Scott et al., 2014). Extreme dry conditions due to deficit rainfall during the growing seasons 2014/15 and 2018/19 (SPI > -1) or wet conditions during the rainy seasons 2010/11 or 2020/21 (SPI > 2) can clearly be observed. These are plotted against MODIS NDVI values showing the distinct seasonality of vegetation greenness during and after the rainy seasons (October to April) and senescence periods during the dry season (May to September). The figure is complemented through selected seasonal representations of rasterized 16-day SPI values based on Copernicus ERA-5 reanalysis data in a 25 km spatial resolution showing distinct spatial-temporal patterns of negative and positive SPI values in the study area, corresponding to calculated SPI values in the graph.

As seen in Figure 6, mean NDVI and precipitation show similar patterns. Both NDVI, as well as

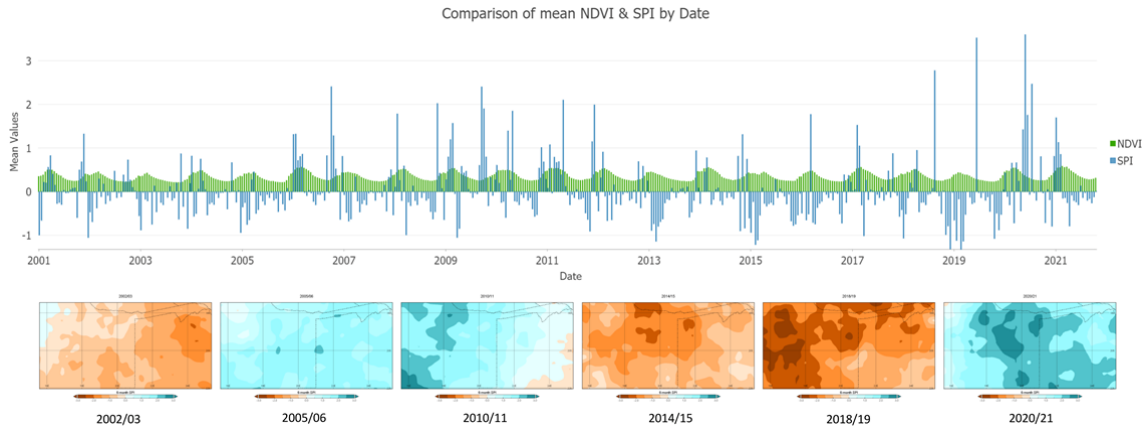


**Figure 5.** Comparison of mean 16-day NDVI and monthly SPI values based on CHIRPS reanalysis and MODIS NDVI data. The selected rasterized representations of SPI for the rainy seasons (shown below) are based on Copernicus ERA-5 reanalysis data and provide good overall spatial-temporal patterns of dryer and wetter conditions.

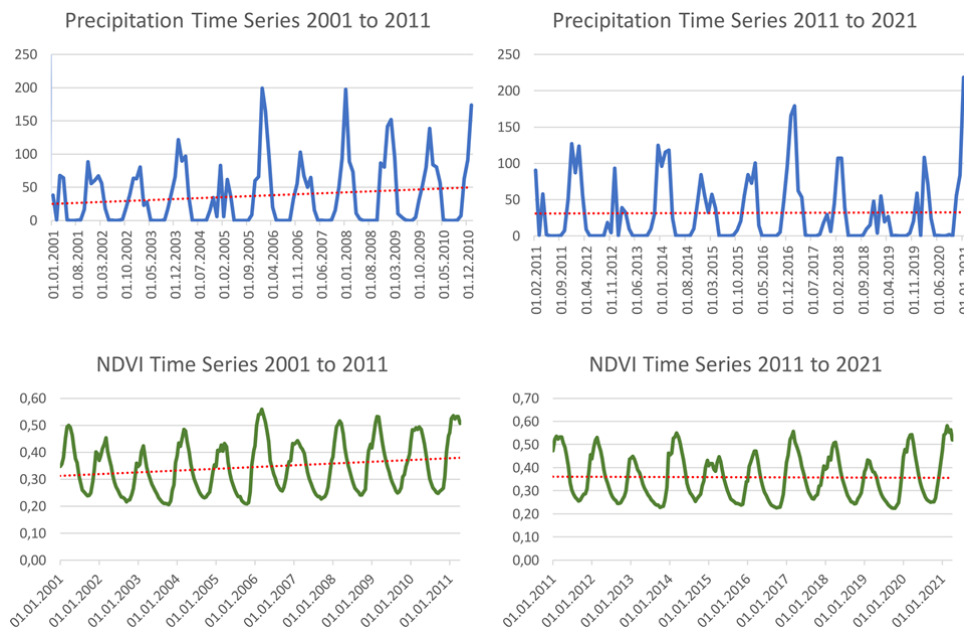


**Figure 6.** Comparison of decadal mean precipitation and NDVI values for the study area (2001 to 2011 and 2011 to 2021).

precipitation increased slightly from 2001 to 2011 but show a slight downtrend in the second decade (2011 to 2021). The mean NDVI values during the rainy seasons range between 0.3 and 0.5. The highest mean NDVI values greater than 0.5 were recorded in 2006, 2011, 2017, 2020, and 2021. Mean NDVI values during the dry season range from 0.2 to 0.25, and increased to 0.28 during the dry season of 2021. 2013 marks the beginning of the perennial drought phase which lasted until 2016. During this period, vegetation was unable to fully recover in subsequent growing seasons, having a significant impact on Namibian ecosystems. A similar pattern can be found for the two-year period from 2018 to 2020, which was marked by extremely dry

conditions. The mean values for the past 20 years (2001 to 2021) contained in both Figures 5 and 6 show no significant trend towards a drier or wetter climate, and would need longer-term statistical time series analysis, based on freely available information on vegetation phenology (that is, AVHRR NDVI) which is particularly favorable due to the long temporal resolution reaching back to 1981.

Figure 7 shows the comparison of VCI, TCI, and ERA-5 precipitation data during the growing season covering a time-span of 10 years (2011/12 to 2020/21). After calculation, VCI, TCI, and VHI have a value range from 0 to 100 with values below 10 classified as extreme drought, from 10 to less than 20 as severe

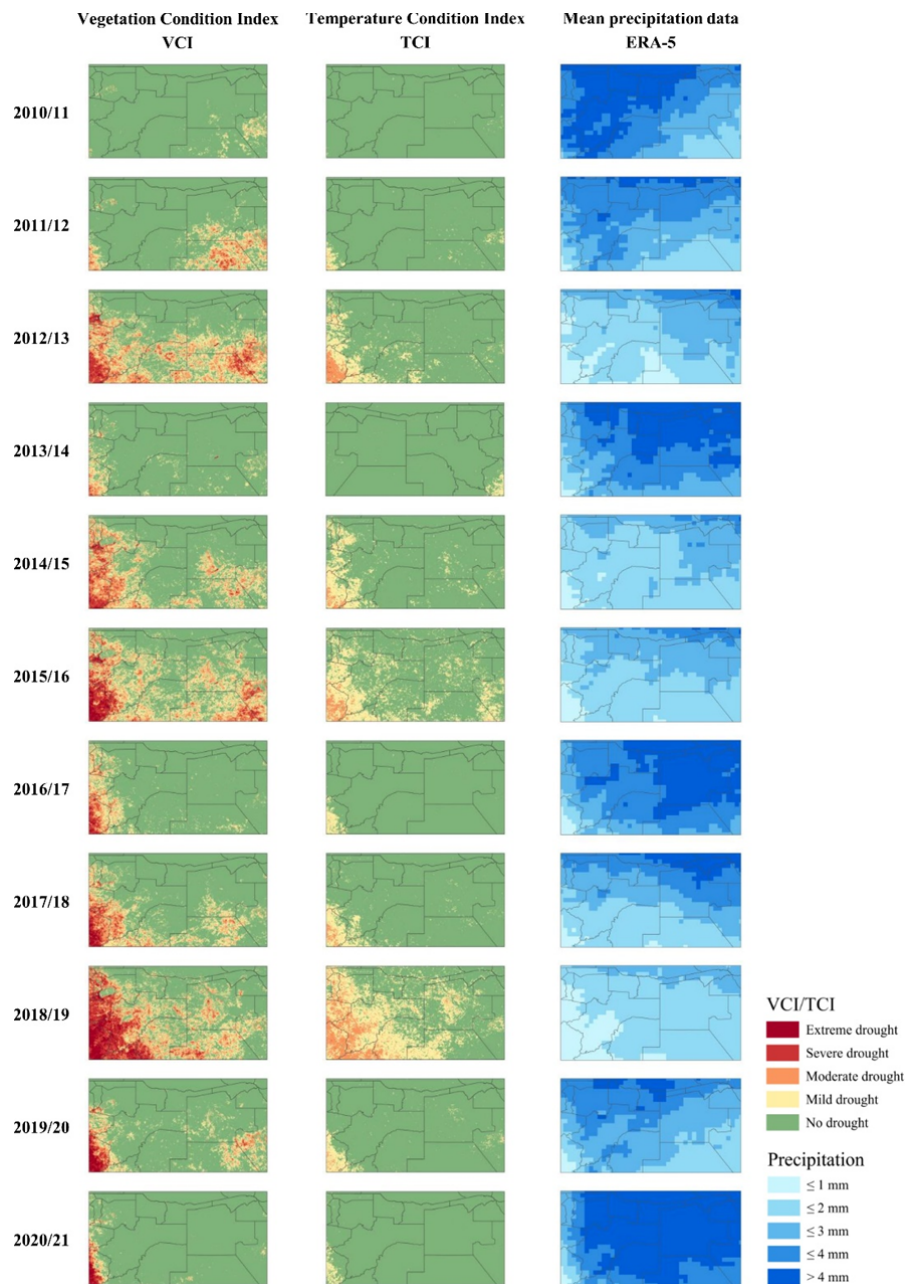


**Figure 7.** Side by side representation of seasonal VCI, TCI and ERA-5 reanalysis data for the 10-year period 2010/11 until 2020/21.

drought, from 20 to less than 30 as moderate drought, from 30 to less than 40 as mild drought, and values above 40 classified as non-drought (Winkler et al., 2017). The ERA-5 data shows classified spatial distribution of average 6-month precipitation values in mm during the respective growing seasons.

The time-series visualization depicts the spatial variation of drought affecting vegetation (VCI) and temperature-related vegetation stress caused by decreased soil moisture (TCI). The figure indicates that drought is a frequent phenomenon during most growing seasons. According to the affected area and severity,

the drought of 2018/2019 was most severe in terms of spatial extent and drought intensity, followed by the drought in 2015/2016 marking the end of the perennial drought phase. The 2018/19 drought event was followed by a precipitation recovery during the 2019/20 and especially the 2020/21 growing seasons, with seasonal VCI and TCI returning to pre-2018 levels. The growing season of 2010/2011 shows the lowest drought severities due to the receipt of above normal rainfall. The figure also shows that drought magnitudes increased after previous drought occurrences due to continued high temperatures and below-average rainfall

over a two-year period. This is true for the seasons 2011/12 through 2012/13, 2014/15 through 2015/16, and 2017/18 through 2018/19. Furthermore, spatial-temporal analysis shows that VCI and TCI exhibit similar patterns, but VCI exhibits significantly higher drought sensitivity in terms of spatial extent and severity levels. During the extreme drought of 2018/19, approximately 5% of the study area was characterized by extreme drought, with 15% characterized as severe and 20% as moderate drought. These areas were predominantly located in the southwest, covering large extents of the Erongo region, western parts of the Otjizondjupa region, and the Khomas region east of Windhoek. Droughts of varying severity can also be found in the Oshana and Oshikoto regions surrounding the Etosha saltpan, as well as the Kunene region. During the growing season of 2015/16, the spatial patterns of drought were similar but less intense, with 2% classified as extreme, 6% as severe, and 13% as moderate, respectively.

The 2012/13, 2014/15, and 2015/16 growing periods also indicate severe and moderate drought expressions in the southeastern parts of the study area, especially in the North-West, Ghanzi and Central regions of Botswana.

Drought severity depicted through TCI was significantly lower with droughts being classified as mild to moderate during all the growing seasons. Lower TCI values indicate temperature-related vegetation stress, which causes a decrease in soil moisture. Vegetation stress is particularly severe where drier soils prevail, particularly in the study area's southwestern corner. Both VCI and TCI have a strong correlation with precipitation data (ERA-5) and follow the typical precipitation gradient, with the highest mean rainfall amounts in the study area's north and northwest. Apart from smaller areas classified as mild drought areas during the 2015/16 and 2018/19 seasons, these areas were predominantly drought free. As such, vegetative drought depicted through VCI can be seen as a manifestation of meteorological drought. Results clearly indicate that vegetation is especially affected by drought if it is preceded by another drought year. Similarly, a particularly wet year stimulates vegetation activity during the following year. Figure 8 shows a side by side representation of the combined drought indices VHI, TVDI and DSI. VHI, which combines VCI and TCI, takes into account vegetation greenness as well as thermal conditions of vegetation and can thus characterize drought conditions more comprehensively during growing seasons with high temperatures.

VHI uses the same classification scheme as VCI and TCI with a threshold of 40% to separate drought from non-drought-prone areas. As equal weights of 0.5 were applied, the time series of VHI displays the combined index values of both components, leading to reduced seasonal drought severity levels compared to VCI. Therefore, no extreme drought was calculated for the 2018/19 growing season. In 2018/19, approximately 5% of the study area was characterized by severe drought, 15% as moderate, and 25% as mild drought, respectively.

The TVDI was classified using the value ranges provided by (Lu et al., 2007), allowing for the estimation of regional soil moisture based on the relationship between NDVI and LST values. Compared to VHI and DSI, TVDI is not based on time series calculations (reference period of 20 years), and only represents the annual range of index values for each growing season. However, spatial patterns of moderate drought correspond well to VHI-classified moderate and severe droughts, which also include LST values. Wet conditions representing higher soil moisture contents can be found along the Okavango delta, around the Ngweze river catchment area bordering Botswana in the Zambezi region and within the Otavi triangle south of Tsumeb. The Otavi mountains, reaching elevations up to 2100m over sea level, cause over-average annual rainfall providing opportunities for large-scale arable farming. These are clearly visible in the 2010/11 and 2011/12 seasonal representations with higher mean precipitation rates. Hotspots of extreme drought conditions indicating extremely low soil moisture conditions can be seen during the years 2012/13, 2014/15, 2015/16, and especially during the 2018/19 growing season. Hotspots include the Etosha salt pan, southern areas of the Oshana region, as well as southwestern areas of the Erongo region.

DSI is a more complex index that adds the normalized ratio of potential and actual evapotranspiration to standardized NDVI values to assess vegetation response to drought. The dimensionless index values were classified into five classes for comparison with VCI, TCI, and VHI, according to (Mu et al., 2013), including extremely dry, dry, average, wet, and extremely wet conditions. The visual interpretation of DSI shows extremely dry conditions during the growing seasons of 2012/13, 2014/15, 2015/16 and especially in 2018/19, depicting drought-prone seasons but showing higher fluctuations and varying spatial patterns in comparison to VHI. Extremely dry conditions depicted through DSI correspond best to severe and moderate drought classes of VHI in 2012/13, 2015/16, and 2018/19 but extend into vegetative areas in the northern parts of the study area including open woodlands, shrubland-woodland mosaics and riparian vegetation along the fringes of the Okavango delta, characterized through higher evapotranspiration rates and less terrestrial water availability during periods of below normal precipitation and high temperatures.

Using the 25 km grid points, index values were extracted for the 10-year time series for further spatial and statistical analysis. The calculation of mean decadal index values, including information on latitude and longitude, allows a generalised representation of spatial distributions as seen in the histograms contained in Figure 9. VCI, TCI as well as combined VHI show distinct patterns of steady latitudinal increase from North (-17°) to South (-22°), and a slight longitudinal increase of drought intensity from East (25°) to West (16°), with index values decreasing significantly from 18° longitude onwards. The indices follow the predominant rainfall gradient and correspond

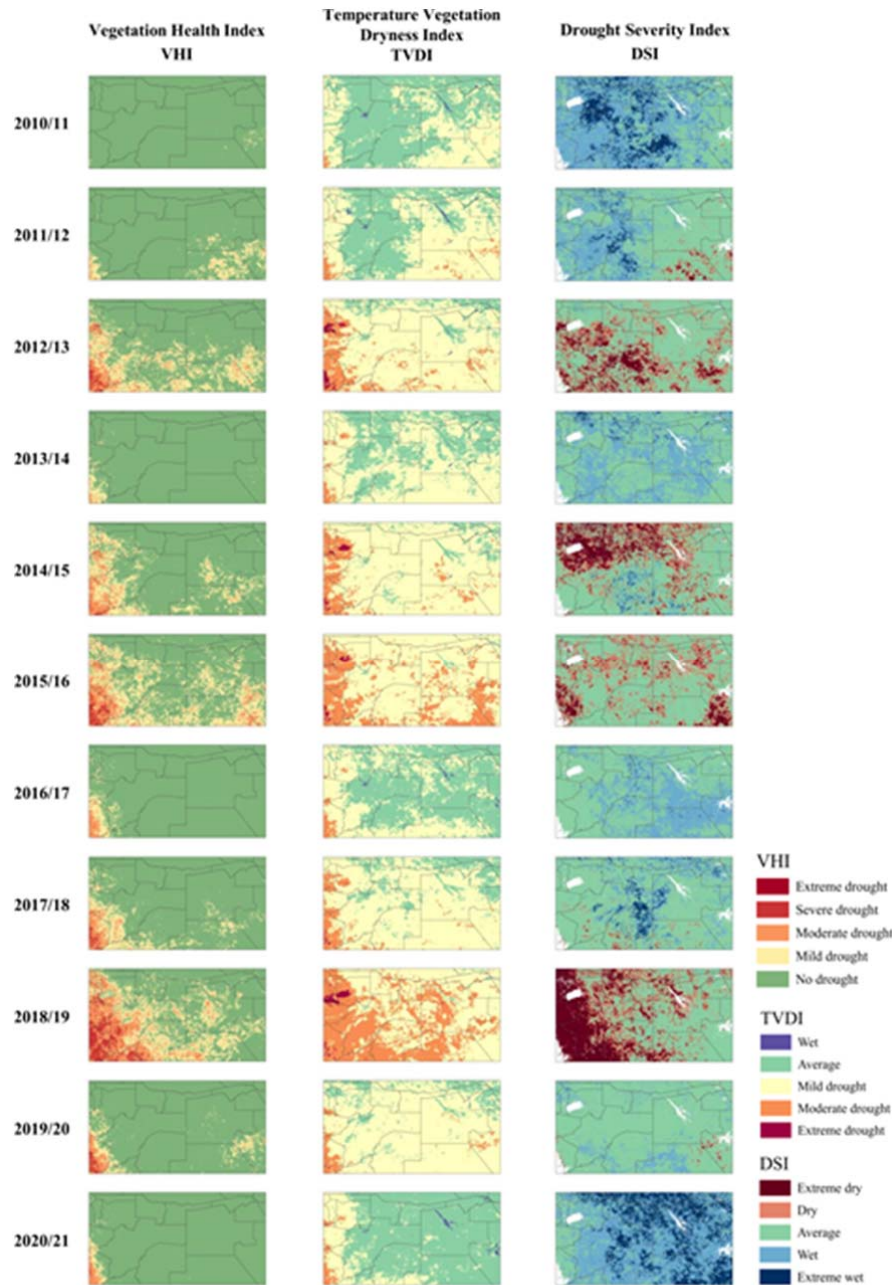


**Figure 8.** Side by side representation of seasonal VHI, TVDI and DSI for the 10-year period 2010/11 until 2020/21.

strongly to ERA-5 precipitation values showing comparable longitudinal and latitudinal values. Thus, higher precipitation values in the north-eastern parts of the study area lead to a higher level of vegetation vitality and less drought severity. The combined indices DSI and TVDI, which include ET, PET, and LST in addition to NDVI, show greater temporal and spatial fluctuations in drought intensity over the course of ten growing seasons (Figure 8). However, mean decadal values of both DSI and TVDI only show slight latitudinal and longitudinal changes in Figure 9, indicating that

drought occurrences were more evenly distributed across the study area. DSI slightly decreases and TVDI slightly increases from East to West indicating slightly dryer conditions and a decline of soil moisture content respectively.

Figure 10a shows the amplitude and temporal characteristics of averaged drought indices during the last decade. For better comparison, TVDI values were multiplied tenfold and show a reversed trend compared to other indices due to the value scale

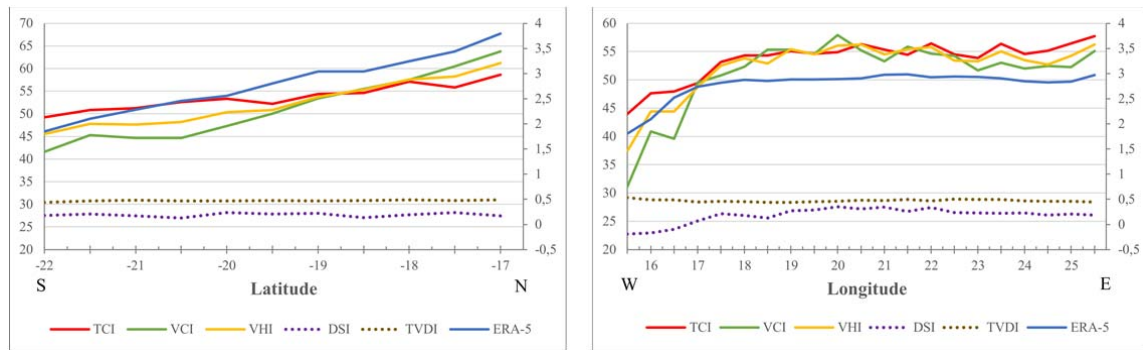


**Figure 9.** Latitudinal and longitudinal change of index values (TCI, VCI, VHI, DSI, TVDI and ERA-5). The primary Y-Axis displays index values for TCI, VCI, VHI and DSI. The secondary Y-Axis represents TVDI, DSI and ERA-5 values.

definition. TVDI values indicating high soil moisture contents correspond to high values of TCI, VCI, and VHI, representing drought-free conditions. The time series comparison indicates that TCI, VCI, VHI, and DSI show similar amplitudes throughout the growing seasons and correspond well with ERA-5 precipitation data. Vegetation, health, temperature related vegetation stress, and terrestrial water availability were lowest during the extreme drought season of 2018/19, followed by 2015/16 and 2012/13, respectively. Water availability with positive effects on vegetation health was highest in 2020/21, followed by 2010/11, 2016/17, and 2013/14, respectively. TVDI as a proxy for soil moisture shows a slightly different tendency, indicating the periods of 2014/15 and 2017/18 as particularly dry. The reason for TVDI deviation is most probably an effect of the calculation method. Whilst the other indices refer to a reference period of 20 years, TVDI only represents the annual seasonal values of LST and NDVI. It should also be noted that the representation of mean values does not reflect region-specific or inter-seasonal differences within the study area.

Figure 10b shows the spatial extent of moderate to extreme droughts in percent of total area recorded through TCI, VCI, and VHI, as well as dry and extremely dry conditions represented through DSI. Amplitudes correspond to the time series in Figure 10a. Highest extents were recorded during the 2018/19 growing season with 52% (DSI), followed by 49% (VCI), 46% (VHI), and 45% (TCI), respectively. The growing season of 2010/11 was pretty much drought-free with coverage of 3% (VCI), 0.4% (VHI), 0.2% (TCI), and 0.05% (DSI). It is also clear that, with the exception of 2014/15, VCI outperforms all other indices, with a second highest spatial extent of 47 percent in 2015/16, followed by 43% in 2012/13.

The selected scatter plots containing coefficients of determination (Figure 11) indicate that seasonal VHI shows the highest correlation with all other indices and ERA-5 precipitation data. VHI exhibits the highest positive correlation with ERA-5 precipitation data with an  $R^2$  value of 0.61 followed by  $R^2$  values of VCI against ERA-5 (0.58), TCI against ERA-5 (0.36), and DSI against ERA-5 with no association between the two

variables (0.05). VHI also exhibits a significant and overall highest correlation with VCI ( $R^2$  value of 0.81) followed by TCI (0.65), TVDI (0.55), and DSI (0.25), respectively.

Correlations show that vegetation-based indices (VCI, VHI) show a generally high correlation with ERA-5 data and that the combined indices TVDI and DSI show less significant correlations against other indices and amongst each other, with an  $R^2$  value of only 0.23 (not contained in Figure 11). DSI performs worst among the combined indices in terms of correlation. It is also noticeable that VCI and TCI only show a correlation of about 33%. However, it is important to state that the correlation analysis using mean values of the entire decade has an effect on correlation results. A year-to-year or inter-annual comparison may present more reliable results.

Figure 12 illustrates the accumulated number of droughts on pixel level during the past decade using pixels classified as moderate to extreme drought through VCI, TCI and VHI as well as dry and extremely dry conditions classified through DSI. TVDI was excluded as the index is not based on a comparable reference period of 20 years.

The quantitative representation clearly indicates the distribution of drought-prone areas, allowing the identification of hotspots. The drought numbers were classified into five classes ranging from  $\leq 5$  to  $< 40$ . Pixel values of 40 indicate that all four indices recorded drought during each growing season within the 10-year time-period. The highest calculated pixel value is 37, falling within the class  $\geq 26$  to  $< 40$ , representing the highest class of re-occurring droughts within the study area with a spatial extent of approximately 15.500 km<sup>2</sup>. Affected areas cover large parts of the Erongo region, especially the south-eastern and western areas around the Erongo mountains, representing granite intrusions with a maximum height of 2350 m over sea level. According the ESA Copernicus Land Cover classification, the dominant land cover types within this class are herbaceous vegetation and bare land, characterized through dry soils and high land surface temperatures.

A second hotspot is located west of the Etosha salt

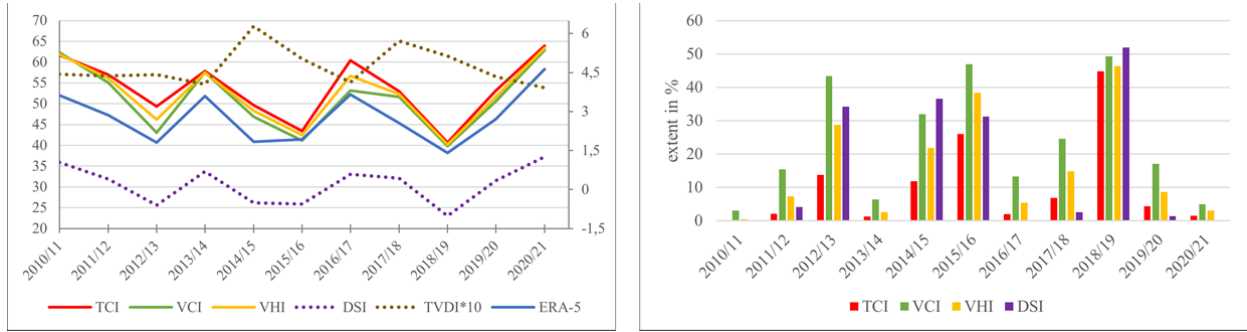


**Figure 10a, b.** Time series of seasonal averaged index values (TCI, VCI, VHI, DSI, TVDI and ERA-5) for the growing periods 2020/2011 until 2020/2021. The primary Y-Axis displays index values for TCI, VCI, VHI and DSI. The secondary Y-Axis represents TVDI, DSI and ERA-5 values (left) and 10b (right): Histogram of spatial extent in percent of all recorded moderate to extreme drought events (right).

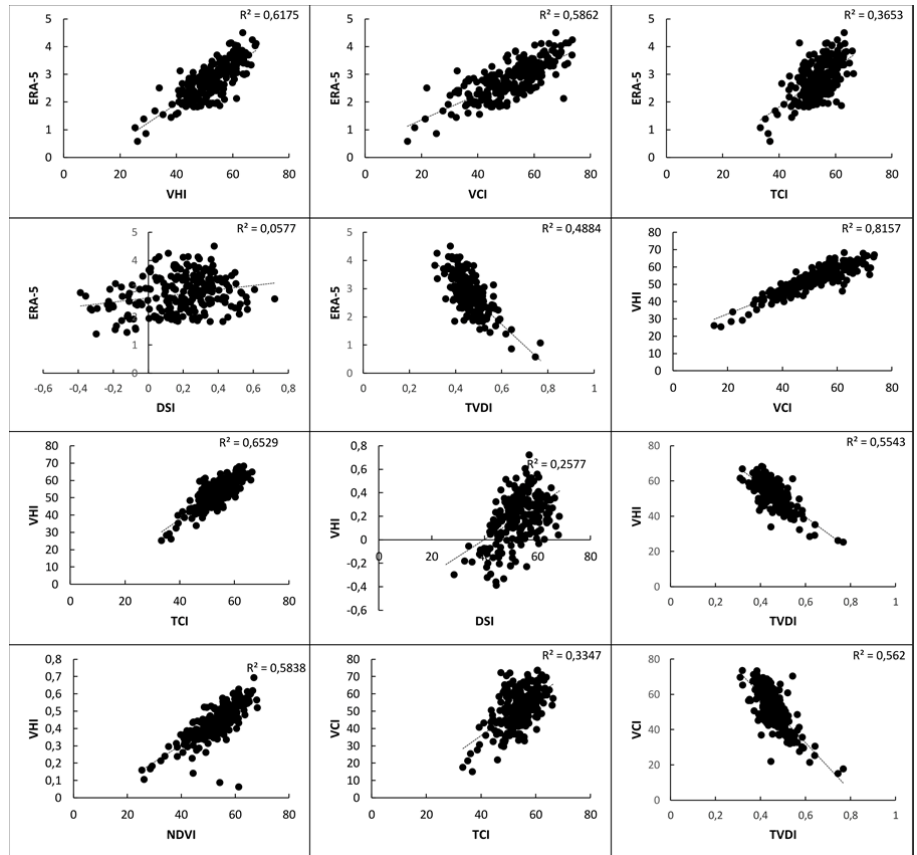


**Figure 11.** Cross-correlation analysis of selected indices and ERA-5 Reanalysis data.

pan where herbaceous vegetation is dominant. The second highest class from  $\geq 16$  to  $\leq 25$  droughts per pixel covers a larger area of approximately 60.000 km<sup>2</sup>. The area covers larger extents of the Khomas region around Windhoek, southwestern parts of the Otjonzondjupa region as well as Kunene and southern parts of the Oshana region. In these regions dense shrubland dominates with an impact on forage availability during drought events that challenges

sustainable farming practices with either livestock or game. These areas extend into the northern Oshana and Omusati regions as part of the Etosha Cuvelai System, characterized by a mosaic of herbaceous vegetation, bare land (Oshanas) and cultivated areas where subsistence agriculture is predominant. Other hotspots are visible south-west of the Okavango delta, where dense shrubland and partially open woodlands dominate, and around the Makadikgadi salt pans with



cumulative process. Greening, on the other hand, which can occur as a result of abundant rainfall during the growing season, does not clearly indicate declining drought conditions and must be interpreted with caution (Liu and Zhou, 2021; Thompson, 2021; Polk et al., 2020). In Namibia, for example, due to droughts and declining livestock numbers, there is continuous bush encroachment, which appears as greening (Mendelsohn, 2002). However, rather than being a "good sign," bush encroachment is part of a degradation process that causes nutrient depletion in soils and further desertification.

DSI, as a proxy for terrestrial water availability, showed comparable seasonal drought amplitudes but different spatial distributions of drought stress. This is reflected in the results of cross-comparison with other indices and ERA-5 rainfall estimates, where DSI showed the lowest coefficients of determination ( $R^2$ ) followed by TVDI. Nevertheless, proxies on water availability and soil moisture have relevance and need to be considered for better comprehension and assessment of droughts and their effects on the environment. The decadal time series analysis (Figures 7 and 8) indicate certain patterns of drought with a clear increase of drought magnitude if droughts are followed by subsequent droughts. However, aspects of post-drought recovery, influenced by drought duration, frequency, post-drought wetness and bioclimatic settings, lack research in Namibia and have definite potential for future investigations.

The accumulated number of droughts through combination of drought indices (Figure 12) can only provide a generalised visualisation of drought hot-spots due to the resampled medium resolution of 500 m pixel size. In addition, the use of seasonal averaged indices, excluding inter-seasonal analysis on a monthly basis, adds to simplification. Another disadvantage is that MODIS satellite data and value-added products have only been available from the year 2000 onwards. This is a relatively short time and counteracts the significance of statistical analyses, making it difficult to link the derived indices to patterns of climate change. The spatial resolution of MODIS also limits the possibility of identifying different vegetation types and their phenological phases. Therefore, time-series of higher resolution imagery has large potential for the detailed evaluation and assessment of drought magnitude, duration and impact on different land cover and vegetation types within the identified drought hotspots. The computation of indices in higher resolution and smaller time steps can provide more detailed information on inter-seasonal variations of drought magnitude and duration and can provide a basis for regional drought preparedness and future drought risk reduction strategies in Namibia.

Considering spatial, temporal, and spectral characteristics, the freely available Copernicus Sentinel-2 data products in resolutions of 10, 20 and 60 m, depending on spectral bands, have high potential to analyze intra- and inter-annual variations in vegetation biomass during vegetation and senescence periods. Lately, much research has been conducted to evaluate

the potential of Sentinel-2 multispectral imagery in assessing drought through vegetation characteristics; soil moisture, evapotranspiration, surface water, and land use/land cover analysis (Varghese et al., 2021; Xijia et al., 2020; Urban et al., 2018). The multispectral imagery allows the retrieval of essential biophysical variables such as LAI and absorbed photosynthetically active radiation (FAPAR) as key quantities in carbon cycle estimation. Sentinel-2 also allows calculation of additional vegetation and drought indices based on the available red-edge bands, providing key information on the vegetation condition which can be used for grassland, forage, and crop monitoring on various scales. Similar results can be achieved using commercial RapidEye imagery in an even higher spatial resolution of 6, 5 m, or the new Landsat 9 sensor with moderate spatial resolution of 15, 30 and 100 m, depending on the spectral band. Landsat 9 will become freely available in the first quarter of 2022, and will be placed in an orbit that it is eight days out of phase with Landsat 8 to increase temporal coverage of observations [www.usgs.gov].

The derived drought indices TCI and TVDI provide proxies of soil moisture. Unfortunately, no comprehensive national network of soil moisture in-situ monitoring instruments providing seamless information exists in Namibia. Future integration of remotely-sensed information on soil moisture and cross-comparison to derive drought indices would therefore definitely add value. For this purpose, ESA SMOS data (Soil Moisture and Ocean Salinity mission), providing spatial-temporal information on soil moisture in a resolution of 35 to 50 km since 2010, has high potential for further research on regional and supra-regional levels. Lately, a new soil moisture agricultural drought index called SMADI, combining SMOS with MODIS NDVI and LST data, has been developed and applied for drought analysis specifically in arid and semi-arid regions (Souza et al., 2021; Sánchez et al., 2018). The additional installation of terrestrial *in-situ* soil moisture and LST sensors in selected areas would add additional value by allowing *in-situ* comparison and validation with sensor-derived drought products such as SMADI, VHI and DSI.

Currently, no single institution in Namibia provides early warning information. Early warning is seen as a coordinated task by different institutions such as MAWF, NMS, and MET. Climate change will necessitate improved and more comprehensive drought mitigation and adaptation strategies in order to improve food security and reduce poverty in the country. These strategies are incorporated into Namibia's National Climate Change Strategy and Action Plan (NCCSAP), and they are critical components of Namibia's long-term national development strategy (Vision, 2030). Aside from the previously mentioned national rangeland monitoring project, there are a couple of regional projects worth mentioning that deal with rangeland assessment or grassland restoration. The NamTip project, led by the University of Bonn and the Namibian University of Science and Technology (NUST), is currently investigating so-called tipping points in

ecosystems caused by changing environmental conditions, such as droughts during growing seasons combined with increasing land use pressure, which can lead to irreversible desertification processes in dryland ecosystems ([www.namtip.uni-bonn.de](http://www.namtip.uni-bonn.de)). The project employs an interdisciplinary approach that includes socioeconomic studies, communication strategies, and in-situ monitoring of forage grass biomass within selected test plots. These are located south of the Waterberg plateau in the Otjozondjupa region (southeast) of Otjiwarongo, an area characterized by successive drought events over the last decade, as shown in Figure 12. A second area of interest with high research potential is the ProNamib nature reserve which was established in 2020. The nature reserve is located outside of the study area in south-western Namibia, representing an ecological transition zone between the eastern edge of the Namib Desert and the Nubib Mountains. ProNamib aims at further land acquisition in order to facilitate seasonal migratory wildlife routes and protect biodiversity. Grassland restoration, achieved through the free movement of animals into areas with higher levels of precipitation, is an important aspect of biodiversity conservation in this area, particularly given the decline in biomass over the last eight years of perennial and extreme drought events. The restoration of historic grazing is expected to result in a significant increase in biomass in the coming years (<https://pronamib.org/>).

## Conclusion

By comparing various MODIS-derived indices and their spatial-temporal dynamics, the study demonstrated the potential of MODIS-based agricultural drought indices in providing a synthesized evaluation of drought events. The study also found that combined indices based on vegetation vitality and land surface temperatures are more appropriate for semi-arid areas than individual parameter indices. The results provide a generalised but consistent basis for further research and development of regionally adapted drought indicators for monitoring and early warning in the semi-arid regions of Namibia. The potential integration of multi-sensor and multi-scale approaches to monitor intraseasonal drought and vegetation responses within identified drought hot spots in the future is highly relevant. Regional and local projects should further integrate detailed biophysical information, such as vegetation phenology, soil characteristics, and high resolution digital elevation models to model surface water runoff and infiltration as well as detailed information on predominant land use. These parameters are central to the further development of drought monitoring systems for Namibia. The additional inclusion of socio-economic information such as agricultural productivity, health related aspects and environmental vulnerability could lead to a new complex and holistic index to support informed decision-making on regional as well as local levels. The handling of such 'Big Data' for time series and trend

analysis is a continuous challenge, especially within developing countries. Thus, adapted and sustainable methods to automate data processing and information dissemination strategies are needed. The continuous development and provision of free and open source software and tools already provide opportunities for capacity development, which should be purposefully integrated into postgraduate courses offered at universities in Namibia and the SADC region, accompanied by regional training workshops to integrate relevant stakeholders and contribute to awareness raising.

The high precipitation rates during the last growing season 2020/21 resulted in the filling of water reservoirs behind dams and an overall improvement in vegetation health across the country. According to NMS, most parts of the country are expected to receive normal to above-normal rainfall during the current 2021/2022 rainy season, indicating stable conditions for further recovery following the previous extreme drought event in 2018/19. However, it is possible that the periodic El Niño- und La Niña effects could cause the next agricultural drought in 2022/23, following the expected three-year drought pattern. This stresses the importance of regionally adapted drought monitoring systems, as well as the implementation of continuous and sustainable drought adaptation and mitigation strategies in Namibia.

## CONFLICT OF INTERESTS

The authors have not declared any conflict of interests.

## REFERENCES

- Ali S, Tong D, Xu Z, Henchiri M, Wilson K, Siqi S, Zhang J (2019). Characterization of drought monitoring events through MODIS- and TRMM-based DSI and TVDI over South Asia during 2001–2017. In: *Environmental Science and Pollution Research International* 26(32):33568–33581.
- Angearu CV, Ontel I, Boldeanu G, Mihailescu D, Nertan A, Craciunescu V, Catana S, Irimescu A (2020). Multi-temporal analysis and trends of the drought based on MODIS data in agricultural areas, Romania. In: *Remote Sensing* 12(23):3940.
- Anyamba A, Tucker CL (2012). Historical perspective of AVHRR NDVI and vegetation drought monitoring. In: *Remotes sensing of drought: Innovative monitoring approaches* 23.
- Buchhorn M, Smets B, Bertels L, Roo B, Lesiv M, Tsendbazar N (2020). Copernicus Global Land Service: Land Cover 100m: collection 3: epoch 2019: Globe.
- Dalezios N, Gobin A, Tarquis A, Eslamian S (2017). *Agricultural Drought Indices: Combining Crop, Climate, and Soil Factors. Handbook of Drought and Water Scarcity: Principles of Drought and Water Scarcity.*
- Du T, Bui D, Nguyen M, Lee H (2018). Satellite-Based, Multi-Indices for Evaluation of Agricultural Droughts in a highly dynamic tropical catchment, Central Vietnam. *Water* 10(5):659.
- Engelhardt M (2021). *Spatial Analysis of Precipitation Time Series over the Okavango-Omatako River Basin based on Reanalysis Data.* Unpublished bachelor thesis Department of Cartography, GIS & Remote Sensing; Georg-August-Universität Göttingen (GAU), Germany.
- Funk C, Peterson P, Landsfeld M, Pedreros D, Verdin J, Shukla S, Husak G, Rowland J, Harrison L, Hoell, Michaelsen J (2015). The climate hazards infrared precipitation with stations – a new environmental record for monitoring extremes. *Scientific Data*, 2, 150066, 2015a.

- Gao F, Zhang Y, Ren X, Yao Y, Hao Z, Cai W (2018). Evaluation of CHIRPS and its application for drought monitoring over the Haihe River Basin, China. *Natural Hazards*, pp. 1-18.
- Gidey E, Dikinya O, Sebego R, Segosebe E, Zenebe A (2018). Analysis of the long-term agricultural drought onset, cessation, duration, frequency, severity and spatial extent using Vegetation Health Index (VHI). *Raya and its environs, Northern Ethiopia. Environmental Systems Research* 7:13.
- Haroon MA, Zhang J, Yao F (2016). Drought monitoring and performance evaluation of MODIS-based drought severity index (DSI) over Pakistan. *Natural Hazards* 84(2):1349-1366.
- Huete A, Didan K, Leeuwen W, Miura T (2011). MODIS Vegetation Indices. In: *Land Remote Sensing and Global Environmental Change: NASA's Earth Observing System and the Science of ASTER and MODIS*.
- Hulley G, Malakar N, Freepartner R (2016). Moderate Resolution Imaging Spectroradiometer (MODIS) Land Surface Temperature and Emissivity Product (MxD21). Algorithm Theoretical Basis Document Land Surface; JPL Publication. [https://lpdaac.usgs.gov/documents/107/MOD21\\_ATBD.pdf](https://lpdaac.usgs.gov/documents/107/MOD21_ATBD.pdf).
- Karnagel A (2020). A comparative Analysis of Drought Indices for Namibia – A Multi-Scale Drought Monitoring Approach. Unpublished master's thesis Department of Cartography, GIS & Remote Sensing; Georg-August-Universität Göttingen (GAU), Germany.
- Karnieli A, Agam N, Pinker RT, Anderson M, Imhoff ML, Gutman GG, Goldberg A (2010). Use of NDVI and land surface temperature for drought assessment: Merits and limitations. *Journal of Climate* 23(3):618-633.
- Karnieli A, Bayasgalan M, Bayarjargal Y, Agam N, Khudulmur S, Tucker CJ (2006). Comments on the use of the vegetation health index over Mongolia. *International Journal of Remote Sensing* 27(10):2017-2024.
- Keyantash J, Dracup JA (2002). The quantification of drought: an evaluation of drought indices. *Bulletin of the American Meteorological Society* 83:1167-1180.
- Kim Y, Lee SB, Yun H, Kim J, Park Y (2017). A Drought analysis method based on MODIS satellite imagery and AWS Data. *IEEE*, pp. 4862-4865.
- Kogan FN (1995). Application of vegetation index and brightness temperature for drought detection. *Advances in Space Research* 15(11):91-100.
- Liu X, Zhou J (2021). Assessment of the Continuous Extreme Drought Events in Namibia during the last decade. *Water* (13):2942.
- Lu Y, Tao H, H Wu (2007). Dynamic Drought Monitoring in Guangxi Using Revised Temperature Vegetation Dryness Index. *Wuhan University Journal of Natural Sciences* 12(4):663-668.
- Luetkemeier R, Stein L, Drees L, Liehr S (2017). Blended Drought Index: Integrated Drought Hazard Assessment in the Cuvélai-Basin. *Climate* 5(51).
- McKee TB, Doesken NJ, Kleist J (1993). The relationship of drought frequency and duration to time scales. *Proceedings of the 8th Conference on Applied Climatology* 17:179-183.
- Mendelsohn J (2002). *Atlas of Namibia. A portrait of the land and its people*. New Africa Books Ltd.
- Mendelsohn J (2009). *Atlas of Namibia. A portrait of the land and its people*. 3 ed. Cape Town: Sunbird Publ.
- Mishra AK, Singh VP (2010). A review of drought concepts. *Journal of Hydrology* 391(1-2):202-216.
- Mu Q, Zhao M, Kimball JS, McDowell N, Running S (2013). A Remotely Sensed Global Terrestrial Drought Severity Index. *Bulletin of the American Meteorological Society* 94(1):83-98.
- Mukherjee S, Mishra A, Trenberth KE (2018). Climate change and drought: A perspective on drought indices. *Current Climate Change Reports* 4:145-163.
- Naumann G, Dutra E, Barbosa P, Pappenberger F, Wetterhall F, Vogt JV (2014). Comparison of drought indicators derived from multiple data sets over Africa. *Hydrology and Earth System Sciences* 18.
- Persend FC (2009). Drought risk analysis using remote sensing and GIS in the Oshikoto region of Namibia. Dissertation, University of KwaZulu-Natal.
- Polk MH, Mishra NB, Young KR, Mainali K (2020). Greening and Browning Trends across Peru's Diverse Environments. *Remote Sensing* 12(15):2418.
- Rensburg P, Tortajada C (2021). An Assessment of the 2015-2017 Drought in Windhoek. In: *Frontiers in Climate, Volume 2, Article: 602962*.
- Republic of Botswana (2012). *Population of Towns, Villages and associated localities*. Department of Government Printing and Publishing Services. Gabarone.
- Rivera JA, Hinrichs S, Marianetti G (2019). Using CHIRPS Dataset to assess wet and dry conditions along the semi-arid central-western Argentina. *Advances in Meteorology* pp. 1-18.
- Running SW, Mu Q, Zhao M, Moreno A (2019). MODIS Global Terrestrial Evapotranspiration (ET) Product (MOD16A2/A3 and Year-end Gap-filled MOD16A2GF/A3GF) NASA Earth Observing System MODIS Land algorithm (for collection 6).
- Sánchez N, González-Zamora A, Piles M, Martínez-Fernández J (2016). A New Soil Moisture Agricultural Drought Index (SMADI) Integrating MODIS and SMOS Products. A Case Study over the Iberian Peninsula. *Remote Sensing* 8(4):287.
- Sandeep P, Reddy GP, Jegankumar R, Kumar KC (2020). Monitoring of agricultural drought in semi-arid ecosystems of Peninsular India through indices derived from time-series CHIRPS and MODIS datasets. *Ecological Indicators* 121:107033.
- Sandholt I, Rasmussen K, Andersen J (2002). A simple interpretation of the surface temperature/vegetation index space for assessment of surface moisture status. *Remote Sensing of Environment* 79(2-3):213-224.
- Sardooi ER, Azareh A, Dameneh HE (2021). Drought monitoring using MODIS Land Surface Products and Normalized Difference Vegetation Index in semi-arid areas of Iran. *Journal of Rangeland Science* 11(4).
- Scott RL, Huxman TE, Barron-Gafford GA, Jenerette GD, Young JM, Hamerlynck EP (2014). When Vegetation Change Alters Ecosystem Water Availability. *Global Change Biology* 20:2198-2210.
- Shikangalah RN (2020). The 2019 Drought in Namibia: An Overview. *Journal of Namibian Studies* 27:37-58.
- Solangi GS, Siyal AA, Siyal P (2019). Spatiotemporal dynamics of land surface temperature and its impact on the vegetation. *Civil Engineering Journal* 5(8):1753-1763.
- Souza AG, Neto AR, de Souza LL (2021). Soil moisture-based index for agricultural drought assessment: SMADI application in Pernambuco State-Brazil. In: *Remote Sensing of Environment* 252:112124
- Tadesse T (2016). Strategic Framework for drought management and enhancing resilience in Africa; [https://catalogue.unccd.int/725\\_White\\_paper\\_second\\_draft\\_Namibia\\_Drought\\_2016.pdf](https://catalogue.unccd.int/725_White_paper_second_draft_Namibia_Drought_2016.pdf).
- Tao L, Ryu D, Western A, Boyd D (2021). A new drought index for soil moisture monitoring based on MPDI-NDVI trapezoid space using MODIS data. *Remote Sensing* 13:122.
- Tesfaye A, Tsegaye T, Berhan G (2021). Spatial and temporal trends and variability of rainfall using long-term satellite products over the Upper Blue Nile Basin. *Remote Sensing in Earth Systems Sciences* 4:199-2015.
- Thenkabail P, Gamage M, Smakhtin V (2004). The Use of Remote Sensing Data for Drought Assessment and Monitoring in Southwest Asia. In: *Research Report 85. International Water Management Institute*. Colombo.
- Thompson S (2021). The effect of long-term climatic trends on vegetation phenology of Namibia's forests and woodlands. Unpublished master's thesis – Namibia University of Science and Technology (NUST).
- Tucker C (1979). Red and photographic infrared linear combinations for monitoring vegetation. *Remote Sensing of Environment* 8(2):127-150.
- Urban M, Berger C, Mudau TE, Heckel K, Truckenbrodt J, Onyango V, Smit I, Schmutz C (2018). Surface Moisture and Vegetation Cover Analysis for Drought Monitoring in the Southern Kruger National Park Using Sentinel-1, Sentinel-2, and Landsat-8. *Remote Sensing* 10:1482.
- Vallejo OM, Negussie KG (2019). Temporal statistical analysis and predictive modelling of drought and flood in Rundu-Namibia. *Climate Dynamics* 53:1248-1260.
- Varghese D, Radulović M, Stojković S, Crnojević V (2021). Reviewing the Potential of Sentinel-2 in Assessing the Drought. *Remote Sensing* 13:3355.
- Vova O, Kappas M, Emam AR (2019). Comparison of satellite soil moisture products in Mongolia and their relation to grassland condition. *Land* 8(9):142.

- West H, Quinn N, Horswell M (2019). Remote Sensing for drought monitoring and impact assessment: Progress, past challenges and future opportunities. *Remote Sensing of the Environment* 232:1-14.
- Winkler K, Gessner U, Hochschild V (2017). Identifying Droughts Affecting Agriculture in Africa Based on Remote Sensing Time Series between 2000–2016: Rainfall Anomalies and Vegetation Condition in the Context of ENSO. *Remote Sensing* 9(8).
- Zargar A, Sadiq R, Naser B, Khan FI (2011). A review of drought indices; In: *Environmental Reviews* 19:333-349.
- Zhang X, Yamaguchi Y, Li F, He B, Chen Y (2017). Assessing the impacts of the 2009/2010 Drought on vegetation indices, normalized difference water index, and land surface temperature in southwestern China. *Advances in Meteorology* pp. 1-9.